NAVAL POSTGRADUATE SCHOOL

MONTEREY, CALIFORNIA

THESIS

EXTREME HURRICANE-GENERATED WAVES IN THE GULF OF MEXICO

by

Carlos Alberto dos Santos Fernandes

December 2005

Thesis Advisor: Thomas H.C. Herbers
Second Reader: Edward B. Thornton

Approved for public release; distribution unlimited

THIS PAGE INTENTIONALLY LEFT BLANK

REPORT DOCUMENTATION PAGE		Form Approved OMB No. 0704-0188

Public reporting burden for this collection of information is estimated to average 1 hour per response, including the time for reviewing instruction, searching existing data sources, gathering and maintaining the data needed, and completing and reviewing the collection of information. Send comments regarding this burden estimate or any other aspect of this collection of information, including suggestions for reducing this burden, to Washington headquarters Services, Directorate for Information Operations and Reports, 1215 Jefferson Davis Highway, Suite 1204, Arlington, VA 22202-4302, and to the Office of Management and Budget, Paperwork Reduction Project (0704-0188) Washington DC 20503.

1. AGENCY USE ONLY *(Leave blank)*	2. REPORT DATE	3. REPORT TYPE AND DATES COVERED
	December 2005	Master's Thesis

4. TITLE AND SUBTITLE: Extreme Hurricane-Generated Waves in Gulf of Mexico	5. FUNDING NUMBERS
6. AUTHOR(S) Carlos Alberto dos Santos Fernandes	
7. PERFORMING ORGANIZATION NAME(S) AND ADDRESS(ES) Naval Postgraduate School Monterey, CA 93943-5000	8. PERFORMING ORGANIZATION REPORT NUMBER
9. SPONSORING /MONITORING AGENCY NAME(S) AND ADDRESS(ES) N/A	10. SPONSORING/MONITORING AGENCY REPORT NUMBER

11. SUPPLEMENTARY NOTES The views expressed in this thesis are those of the author and do not reflect the official policy or position of the Department of Defense or the U.S. Government.

12a. DISTRIBUTION / AVAILABILITY STATEMENT	12b. DISTRIBUTION CODE
Approved for public release; distribution unlimited.	

13. ABSTRACT (maximum 200 words) Accurate predictions and understanding of littoral and coastal wave conditions are of major importance to military operations and civilian coastal zone management. Although WaveWatchIII (WW3) is used by many operational forecasting centers around the world, there is a lack of field studies to evaluate its accuracy in regional applications and under extreme conditions, such as Hurricanes.

Data from seven National Data Buoy Center (NDBC) buoys in the Gulf of Mexico, together with an array of pressure and pressure-velocity sensors deployed on the Florida Panhandle shelf during the Office of Naval Research (ONR) SAX04 experiment, were used to test WW3 predictions of extreme waves generated by Hurricane Ivan.

The model predicts large differences between wave conditions on the left and right sides of the hurricane track owing to the difference in "dwell time" between wave propagating against and with the storm. Analysis reveals a tendency to predict smaller wave heights and later arrival of hurricane swell than is observed. Additionally, the default operational setting for dissipation by bottom friction yields too much dissipation on the continental shelf. Overall, the agreement between observations and model predictions is reasonable.

14. SUBJECT TERMS Wave Model; WaveWatch III; Hurricane Ivan; Gulf of Mexico; Depth Induced breaking	15. NUMBER OF PAGES 63
	16. PRICE CODE

17. SECURITY CLASSIFICATION OF REPORT	18. SECURITY CLASSIFICATION OF THIS PAGE	19. SECURITY CLASSIFICATION OF ABSTRACT	20. LIMITATION OF ABSTRACT
Unclassified	Unclassified	Unclassified	UL

NSN 7540-01-280-5500 Standard Form 298 (Rev. 2-89)
Prescribed by ANSI Std. 239-18

THIS PAGE INTENTIONALLY LEFT BLANK

Approved for public release; distribution unlimited

EXTREME HURRICANE-GENERATED WAVES IN THE GULF OF MEXICO

Carlos A. S. Fernandes
Lieutenant, Portuguese Navy
B.S., Portuguese Naval Academy, 1995

Submitted in partial fulfillment of the
requirements for the degree of

MASTER OF SCIENCE IN PHYSICAL OCEANOGRAPHY

from the

NAVAL POSTGRADUATE SCHOOL
December 2005

Author: Carlos Alberto dos Santos Fernandes

Approved by: Thomas H. C. Herbers
Thesis Advisor

Edward B. Thornton
Second Reader

Mary L. Batteen
Chairman, Department of Oceanography

THIS PAGE INTENTIONALLY LEFT BLANK

ABSTRACT

Accurate predictions and understanding of littoral and coastal wave conditions are of major importance to military operations and civilian coastal zone management. Although WaveWatchIII (WW3) is used by many operational forecasting centers around the world, there is a lack of field studies to evaluate its accuracy in regional applications and under extreme conditions, such as hurricanes.

Data from seven National Data Buoy Center (NDBC) buoys in the Gulf of Mexico, together with an array of pressure and pressure-velocity sensors deployed on the Florida Panhandle shelf during the Office of Naval Research (ONR) SAX04 experiment, were used to test WW3 predictions of extreme waves generated by Hurricane Ivan.

The model predicts large differences between wave conditions on the left and right sides of the hurricane track owing to the difference in "dwell time" between wave propagating against and with the storm. Analysis reveals a tendency to predict smaller wave heights and later arrival of hurricane swell than is observed. Additionally, the default operational setting for dissipation by bottom friction yields too much dissipation on the continental shelf. Overall, the agreement between observations and model predictions is reasonable.

THIS PAGE INTENTIONALLY LEFT BLANK

TABLE OF CONTENTS

I. INTRODUCTION 1
   A. BACKGROUND AND MOTIVATION 1
   B. STUDY PURPOSE 2

II. DATA SETS AND METHODOLOGY 5
   A. BUOY DATA 5
   B. SEDIMENT ACOUSTICS EXPERIMENT 2004 (SAX04) - IN SITU INSTRUMENTATION 7
   C. SATELLITE DATA 10

III. WIND FIELD 13
   A. SYNOPTIC HISTORY 13
   B. METEOROLOGICAL MEASUREMENTS 14
   C. WINDS FIELD 15

IV. WAVE MODEL 21
   A. BRIEF DESCRIPTION OF WAVEWATCH III (WW3) 21
   B. GRID SETTINGS 23

V. WAVE MODEL – DATA COMPARISONS 25
   A. DEEP WATER 28
   B. FLORIDA CONTINENTAL SHELF 35

VI. CONCLUSIONS 43

LIST OF REFERENCES 45

INITIAL DISTRIBUTION LIST 47

THIS PAGE INTENTIONALLY LEFT BLANK

LIST OF FIGURES

Figure 1. The Hurricane Ivan track (blue dashed line) and locations of the seven NDBC buoys that measured wind and wave conditions. 5
Figure 2. Geographical location of the nine deployment sites. Contours indicate the Continental Shelf bathymetry at 20m intervals. 9
Figure 3. Sea spider tripod with a PUV sensor in the center. Mounted on the side is an assembly with an acoustic release, used for recovery. 9
Figure 4. Sea spider tripod with a pressure sensor in the center and dual acoustic release recovering systems. 10
Figure 5. Satellite picture of Hurricane Ivan at 16SEP0000Z (from www.noaanews.noaa.gov) 14
Figure 6. Flow chart of procedures used to achieve a wind field (Powell, 1996) 16
Figure 7. Example AOML H-Wind field snapshots during Ivan. The wind field is gridded on a moving “square” of approximately 1000Km by 1000Km centered on the eye of the storm 20
Figure 8. The left column shows the synoptic wind field and the right column the corresponding wave field for Sep. 13 00:00 UTC, 14 00:00 UTC, 15 00:00 UTC, 16 00:00 UTC and 16 09:00 UTC (landfall). White line indicates hurricane track with a red filled circle at the location of the hurricane eye. The white arrows indicate the wind (left panels) and wave (right panels) directions. Colors correspond to wind speed (left panels) and significant wave height (right panels). 27
Figure 9. Comparison of observed (blue curve) and predicted (red curve) significant wave heights at the seven NDBC buoys. 29
Figure 10. Comparison of the observed (blue crosses) and predicted (red crosses) mean wave direction at six NDBC buoys. 31
Figure 11. Two dimensional frequency directional spectra predicted by WW3 at station 42001. a) 15SEP 09:00UTC; b) 16SEP 15:00 UTC. Contours indicate energy levels on a log scale at $10^{1/2}$ intervals relative to the maximum energy. 32

Figure 12. Two dimensional frequency directional spectra predicted by WW3 at station 42003. a) 15 SEP 09:00UTC; b) 16SEP 15:00 UTC. Contours as in previous figure. 32
Figure 13. Comparison of observed (blue curve) and predicted (red curve) peak period at the seven NDBC buoys. 33
Figure 14. GEOSAT FOLLOW ON (GFO) satellite tracks – September 13-16, 2004 34
Figure 15. Comparisons between GEOSAT observations and WaveWatch III predictions along the tracks shown in Figure 14. 35
Figure 16. WW3 Wave field (SWH) predictions for September 15 21:00UTC and September 16, 03:00 and 06:00 UTC 37
Figure 17. WW3 Peak Period field. The Hurricane track is represented by the white line while the red spot indicates the eye of the storm. 38
Figure 18. Comparison between WW3 predictions and observations at SAX04 sites 7 and 9. Blue line – WW3 predictions with dissipation 39
Figure 19. Comparison between WW3 predictions and observations at SAX04 site 5. 40

LIST OF TABLES

Table 1. NDBC buoys used in the study 6
Table 2. Frequencies and bandwidths used on spectral analysis for NDBC buoys 7
Table 3. Geographical position, depth and what kind of sensor was deployed on the 9 different sites 8

THIS PAGE INTENTIONALLY LEFT BLANK

ACKNOWLEDGMENTS

I sincerely thank my advisor, Professor Tom Herbers, for his infinite wisdom and for the way that, since the first day he hosted me, enabling me to achieve such a task. I'm also grateful to Mr. Paul Jessen who was always a pillar assisting me in all the programming problems, while setting and running the WaveWatch III model.

Their advice, support and passion were tremendously important. I particularly want to thank Prof. Herbers for allowing me to be part of the SAX04 experiment recovering cruise. It's always a worthwhile experience to be part of such events.

My thank you is also extensive to Mr. Ardhuin Fabrice who even on the other side of the world never stopped helping me.

Professor Thornton was also an important help. His knowledge and his ability to simplify everything that for me was so complicated were very helpful. Thank you.

I want to express my undying gratitude to my family, especially to my beautiful wife, for her support and encouragement, following me from Lisbon to Monterey, allowing us to enjoy a lifetime adventure. It was simply impossible to fulfill this task without the presence of both of my children, Catarina and Manuel, who were always asking me when I had time to play with them.

THIS PAGE INTENTIONALLY LEFT BLANK

I. INTRODUCTION

Since ancient times, when men decided to explore the unknown sea, wind and waves were always feared and were objects of major interest. In 1490, the great navigator, Count Vasco da Gama, used to spend a significant amount of time per day watching the sea with the purpose of understanding its mysteries, how waves react to wind or the tide effects. Five hundred years later we still spend a considerable amount of time watching and monitoring the sea in quest of the same knowledge.

Due to the present demands of our society, we can not just understand its mechanisms. We also have to be able to predict it. In order to carry out that task, in the last decades sophisticated numerical models have been developed and implemented on high performance computers to provide operational global and regional wave forecasts.

A. BACKGROUND AND MOTIVATION

Forecast models had their beginning with Sverdrup and Munk during the 1940's, based on a semi-empirical wave forecasting relationship that made extensive use of graphic solutions (Sverdrup and Munk, 1947), but it was Gelci in the late 1950's who developed the first wave prediction model using a balance equation between wind input and dissipation. The second generation wave models started in the early 1970's with the Joint North Sea Wave Project (JONSWAP) (Hasselmann et al., 1973). Although an improvement in forecasting capabilities was achieved, this second generation model still had a simplified view of

nonlinear transfer, and did not handle the transition between windsea and swell properly. In 1985, the SWAMP study concluded that none of the existing models were reliable in extreme situations, and in fact, it was proposed that a third generation model should be developed.

Improvements in computational capabilities and numerical methods led to the first third generation wave model WAM (WAMDI, 1988). WAM solves the full spectral energy balance including nonlinear wave-wave interactions. The source function was still represented as a combination of wind input, nonlinear transfer and dissipation, however significant improvements were introduced in the parameterization of the source components.

WAVEWATCHIII (WW3)(Tolman, 2003), another third generation wave model, introduced further refinements product based on the previous models WaveWatch I and II, including a third-order numerical scheme and new formulations of the wind input and dissipation. WW3 is the operational model used at FNMOC for global and regional wave forecasts.

B. STUDY PURPOSE

Natural disasters associated with severe meteorological disturbances are among the most impressive and destructives events. In addition to damage from hurricane-force winds, extreme waves cause beach erosion and property damage. Accurate prediction of waves and associated sediment transport is critical for coastal zone management.

Large waves also affect military operations includeding amphibious landings, mine warfare and military insertions. The extent, to which waves influence so many processes and operations in the marine environment, has driven a need for accurate wave prediction models. Presently, the main forecasting centers are using third generation global wave models, such as WW3. Numerous studies have been performed to validate model predictions with in situ and remote sensing observations, but the accuracy of these models in extreme hurricane conditions is not well understood.

The operational wave prediction model WW3 was designed for global applications with relatively coarse resolution (typically around 1 degree). Its accuracy and stability has been demonstrated through extensive validation with buoy and satellite altimeter measurements (Tolman, 2003). The accuracy of WW3 in regional applications, that requires higher resolution to resolve coastline and bathymetry effects, and the performance of WW3 in extreme meteorological conditions, like hurricanes, is not well known and is the topic of this study.

THIS PAGE INTENTIONALLY LEFT BLANK

II. DATA SETS AND METHODOLOGY

This study focuses on a period of 4 days, September 13 to 16, 2004, when the category V hurricane Ivan crossed the Gulf of Mexico and made landfall on the Alabama coast. Fortunately, at that time the Sediment Acoustics experiment funded by the Office of Naval Research (ONR) took place on the Panhandle coast, providing unique observations of the transformation of extreme hurricane-generated waves across the continental shelf. These data were analyzed together with available data from permanent buoys in the Gulf of Mexico and the Geosat Follow On satellite. The data sets and analysis methodology are described in this chapter.

A. BUOY DATA

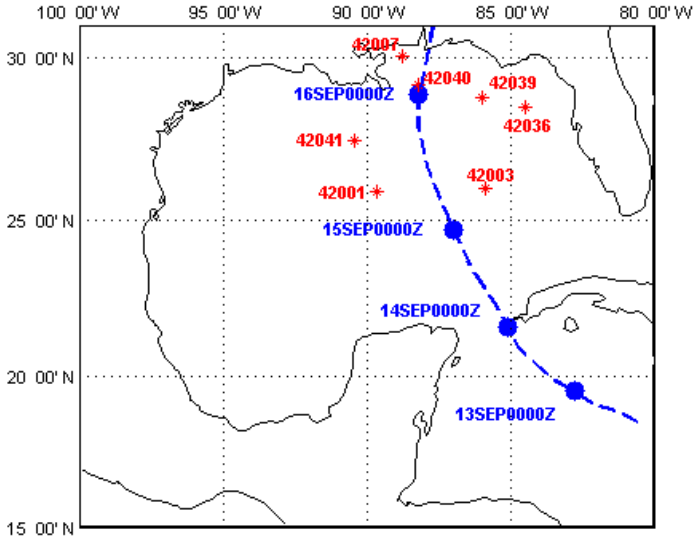

Figure 1. The Hurricane Ivan track (blue dashed line) and locations of the seven NDBC buoys that measured wind and wave conditions.

The buoy datasets used in this thesis were provided by the National Data Buoy Center (NDBC). Wind and wave data were collected by seven buoys in the Gulf of Mexico. The main characteristics and geographical positions of these buoys are listed in Table 1. The buoys are deployed in depths ranging from 14 to 3200 meters (Table 1). Buoys 42003 and 42039 were very close to the hurricane path and recorded extreme wind and wave conditions. Buoy 42040, located along the path was damaged during the passage of the hurricane and stopped collecting data.

Table 1. NDBC buoys used in the study

Buoy	Position (WGS-84) Lat (N)/Lon (W)		Dir	Type	Diameter (m)	Depth (m)
42001	25.90	89.67	Yes	Discus	12	3246
42003	26.01	85.91	Yes	Nomad	6	3233
42007	30.09	88.77	Yes	Discus	3	14
42036	28.50	84.52	Yes	Discus	3	54.5
42039	28.79	86.02	Yes	Discus	3	291.4
42040	29.18	88.21	Yes	Discus	3	443.6
42041	27.50	90.46	Yes	Discus	3	1435

All NDBC buoys are equipped with a suite of commercially available sensors such as anemometers and barometers that provide hourly standard meteorological observations including mean wind speed and direction, maximum gust, barometric pressure, air temperature, and sea

surface temperature. To collect wave data, the buoys are equipped with accelerometers that are used to measure vertical acceleration with a sample frequency of 1.5Hz for 20 minutes. The acceleration time series are integrated twice to form sea surface elevation time series (acceleration back to velocity back to displacement). A Fast Fourier Transform (FFT) is applied to the data by the processor on-board the buoy to transform the data from the temporal domain into the frequency domain (Steele, 1993). Spectral analysis yields wave frequency spectra and standard parameters such as significant wave height (SWH) and peak period (Tp). The spectral data (energy density and directional moments) are computed for 47 frequency bands, in the range of 0.020Hz to 0.485Hz (Table 2).

Table 2. Frequencies and bandwidths used in spectral analysis for NDBC buoys

Frequency (Hz)	Bandwidth (Hz)
0.020 – 0.100	0.005
0.100 – 0.350	0.010
0.350 – 0.485	0.015

B. SEDIMENT ACOUSTICS EXPERIMENT 2004 (SAX04) - IN SITU INSTRUMENTATION

SAX04, an ONR experiment aimed at understanding acoustic propagation through sediments, was conducted off Panama City, Florida from early September through the middle of November of 2004. In addition to an extensive suite of acoustic/geological measurements, 13 wave-measuring instruments were deployed by the Naval

Postgraduate School at 9 different sites (Figure 2), and these data are used in this study. The instrumentation includes 4 Nortek Vector puv sensors (sensors that measure pressure and horizontal velocity, u and v) (Figure 3), 8 pressure sensors (Figure 4), and 1 wavebuoy (Datawell Directional Waverider).

Table 3. Geographical position, depth and type of sensors deployed at 9 different sites

Site	Latitude (N) (WGS-84)	Longitude(W) (WGS-84)	Depth(m)	Sensor
1	30^0 23.395′	86^0 38.388′	12	2 PUVs
2	30^0 18.483′	86^0 07.493′	12	pressure
3	29^0 59.010′	85^0 34.990′	17	pressure
4	29^0 32.710′	85^0 17.237′	15	pressure
5	29^0 46.247′	84^0 28.861′	10	2 PUVs pressure
6	28^0 57.277′	85^0 01.971′	47	pressure
7	29^0 58.053′	86^0 35.724′	83	pressure
8	30^0 13.524′	86^0 37.688′	28	pressure
9	30^0 22.908′	86^0 38.374′	18	wavebuoy

With the exception of the wavebuoy, all moorings consist of a fiberglass tripods (Sea-Spider) on which instruments (PUV or pressure sensor) are mounted. Also attached to the Sea-Spider is an acoustic release with a float assembly, which is used during recovery of the platform and instrument.

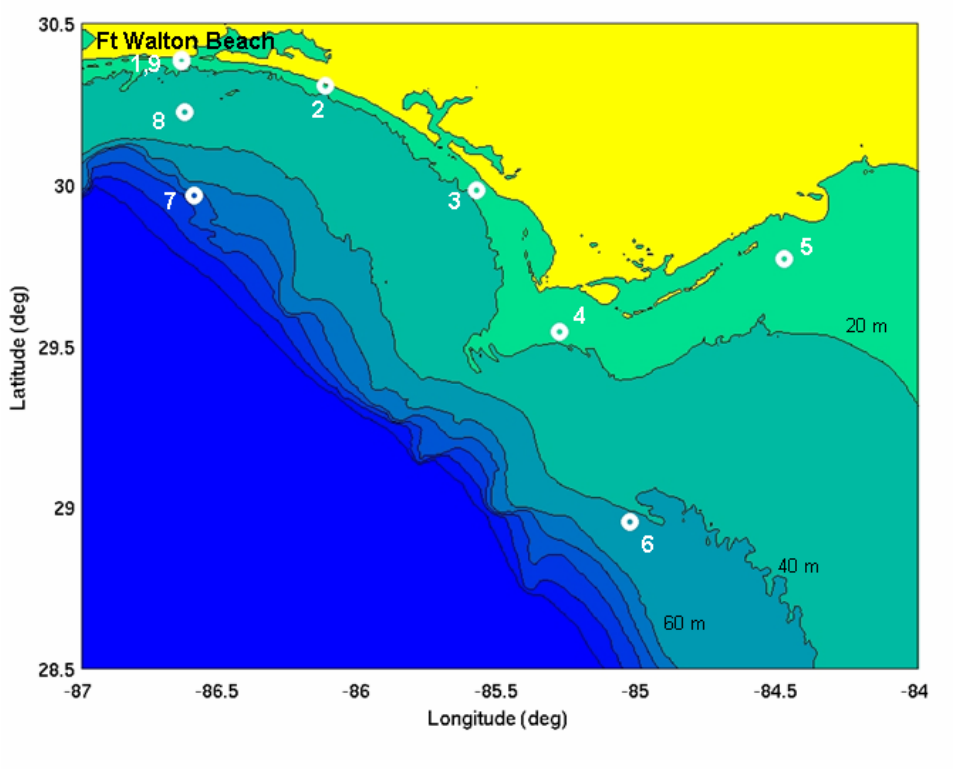

Figure 2. Geographical location of the nine deployment sites. Contours indicate the Continental Shelf bathymetry at 20m intervals.

Figure 3. Sea spider tripod with a PUV sensor in the center. Mounted on the side is an assembly with an acoustic release, used for recovery.

Figure 4. Sea spider tripod with a pressure sensor in the center and dual acoustic release recovering systems.

High quality data were collected at six sites: three to seven and nine. Instrument platforms at sites one, two and eight were lost in the extreme wave conditions of Hurricane Ivan.

C. SATELLITE DATA

The Navy's GEOSAT Follow-On (GFO) satellite was launched on February 10, 1998, following the previous GEOSAT that was disabled in 1990.

GFO is a mini satellite designed and built by Ball Aerospace & Technology Corporation (BATC) of Boulder, Colorado. Its mission is managed by the Meteorological/Oceanographic (METOC) Program Office of Space and Naval Warfare Systems Command (SPAWAR) in San Diego, CA, and its major objective is to provide

operational altimetry data for the US Navy as well as for NOAA, NASA, and University ocean science and ocean monitoring.

A 13.5-GHz radar altimeter is the primary payload, providing wave-height measurements to an accuracy of 3.5cm. The altimeter tracks the radar time delay, with a closed loop adaptive algorithm. If the altimeter transmitted a pulse and waited for the return from the surface, the resulting time delay would be a direct measure of the range to the surface. In order to increase the ocean sampling rate and reduce height noise (bad measurements), the radar has five pulses in the air at any given time, and measures the delay between the most recent pulse generated and the next pulse received (generated 5 pulse intervals ago) and the true range is computed by the Sensor Data Record (SDR) software on the ground at the Payload Operations Center (POC), co-located with the Altimeter Data Fusion Center (ADFC) at Naval Oceanographic Office (NAVOCEANO) at Mississippi (http://Gfo/Data_val/Cal_formats/time_mgt.htm).

THIS PAGE INTENTIONALLY LEFT BLANK

III. WIND FIELD

Hurricane Ivan was a standard Cape Verde[1] hurricane that reached Category 5 strength three times on the Saffir-Simpson Hurricane Scale[2] (SSHS).

A. SYNOPTIC HISTORY

Hurricane Ivan originated from a large tropical wave off the African West Coast on August 31, 2004. Despite a relatively low latitude (9.7°N), development continued and it is estimated that the cyclone became Tropical Storm Ivan just 12 hours later at 0600UTC September 3 (Stewart, 2005)[3].

After emerging over the southern Gulf of Mexico early on September 14, Ivan turned north-northwestward and then northward. As Ivan was getting close to the northern Gulf coast, the upper-level wind flow ahead of the trough became more westerly and strengthened to more than 30kt, which increased the shear and advected dry air into the inner core region. The presence of cooler shelf water just offshore weakened Ivan before making landfall as a 105kt

---

1- Cape Verde type hurricanes are those Atlantic basin tropical cyclones that develop into tropical storms fairly close (<1000 km) to the Cape Verde Islands and then become hurricanes before reaching the Caribbean.

2- The Saffir-Simpson Hurricane Scale is a 1-5 rating based on the hurricane's present intensity. This is used to give an estimate of the potential property damage and flooding expected along the coast from a hurricane landfall. Wind speed is the determining factor in the scale, as storm surge values are highly dependent on the slope of the continental shelf in the landfall region.

3- For more details concerning hurricane Ivan see the following report: Stewart, Stacy R., Hurricane Ivan 2-24 September 2004 - Tropical Cyclone Report, *National Hurricane Center,* 2005.

hurricane (category 3 on the SSHS) at approximately 0650UTC September 16, just west of Gulf Shores, Alabama.

By this time, the eye diameter had increased to 40-50NM (Figure.5), which resulted in some of the strongest winds occurring over a narrow area near the southern Alabama-western Florida panhandle border.

B. METEOROLOGICAL MEASUREMENTS

Observations during Ivan include satellite-based Dvorak[4] technique intensity estimates from the Tropical Analysis and Forecast Branch (TAFB), the Satellite Analysis Branch (SAB) and the U. S. Air Force Weather Agency (AFWA), as well as flight-level and dropwindsonde observations from flights of the 53rd Weather Reconnaissance Squadron of the U. S. Air Force Reserve Command (AFRES).

Figure 5. Satellite picture of Hurricane Ivan at 16SEP0000Z (from www.noaanews.noaa.gov)

4- The Dvorak technique is a methodology to get estimates of tropical cyclone intensity from satellite pictures. Vern Dvorak developed the scheme using a pattern recognition decision tree in the early 1970s.

Microwave satellite imagery from NOAA polar-orbiting satellites, the NASA Tropical Rainfall Measuring Mission (TRMM), the NASA QuikSCAT, and Defense Meteorological Satellite Program (DMSP) satellites were also helpful in monitoring Ivan.

Loaded with sophisticated sensors and weather measuring devices, the different aircrafts were launched every six hours for missions that typically lasted eight to twelve hours. Aircrews usually fly into the building storm at about 10,000 feet above the ocean's surface. During the missions, the aircrafts crisscross the hurricane and release small "dropsonde" canisters. Dropped by parachute, these free-floating sensors provide very accurate measurements of the storm's location and intensity. The canisters relay barometric pressure, wind speed and direction and other details to the aircraft during their descent until they hit water. After checking the data, the crews forward the information directly to the National Hurricane Center.

C. WINDS FIELD

In order to analyze the surface wind field, it is fundamental that all the information conform to a common height. To achieve that, a complex five-step process was developed (Powell, 1996) that is briefly reviewed here.

Step 1 – Compute the mean (10 min average)

The surface boundary layer similarity theory used in steps 2 to 4 requires a mean wind computation. A 10 min mean is used because it is more stable than the raw 1 min mean winds.

Step 2 – Determination of observation exposure type

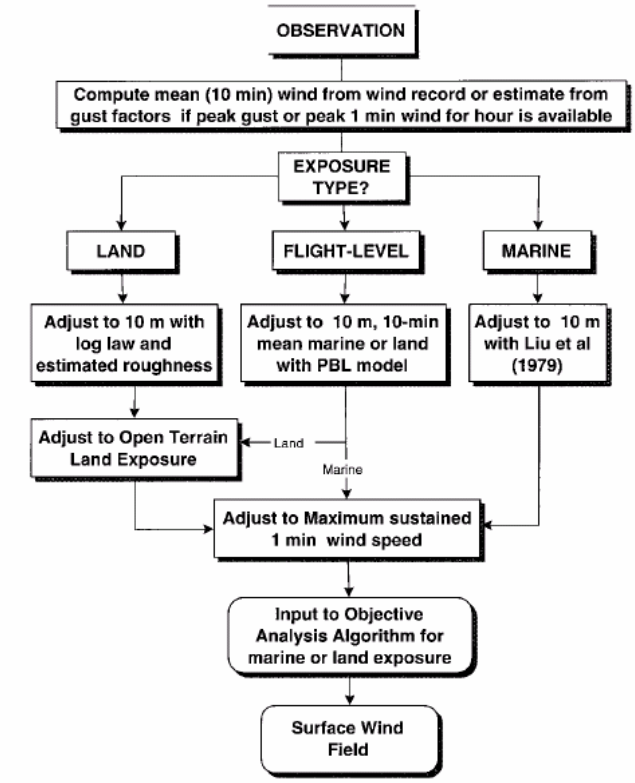

Figure 6. Flow chart of procedures used to achieve a wind field (Powell, 1996)

In this step it is decided what type of fetch is used. The fetch depends upon whether the wind direction is onshore, offshore or alongshore. The land exposure type is

important because wind blowing from sea to land decelerates and forms an internal boundary layer (IBL) whereas wind blowing from land to sea accelerates.

Step 3 – Adjust to the reference height (10 meters)

The World Meteorological Organization (WMO) recommends the wind measurement height to be 10 meters above ground level. The method used to adjust wind speeds to that level is described by Liu et al. (1979). The method iteratively solves equations involving the air-sea exchanges of momentum, heat, and water vapor to arrive at the wind speed profile in the lower atmospheric boundary layer. Air and water temperature, wind speed at the height of observation, and relative humidity are required inputs to the algorithm. Since relative humidity isn't usually measured, it is assumed to be 85%.

Step 4 – Adjust to the reference exposure

In order to simplify the analysis, all the input data over land is converted to an equivalent open ocean exposure environment with a roughness length of 0.03m.

Step 5 – Adjust to the maximum sustained wind over the averaging period

After adjustment to 10m and adjustment to open ocean for land exposures, observations with averaging times greater than 2 min are interpolated to 1 min intervals.

After completion of these standardization steps, the data are processed in an objective analysis scheme, which interpolates data from irregularly spaced locations to a fixed grid. A filtering procedure is applied in which stations surrounding a nearby grid point receive a relative weight, typically based on the distance they lie from the grid point. In this way, the grid point value is not representative of a single station, but is instead a best fit to all the surrounding data. The effect of considering several stations leads to smoothing of the data. The final grid point value will range somewhere between the maximum and minimum values of the stations used.

The Atlantic Oceanographic and Meteorological Laboratory (AOML) generated a final gridded H-Wind field for hurricane Ivan with spatial and temporal resolutions of 0.05° (≈6Km) and 3 hours respectively that was used in this thesis. The mobile grid is centered on the eye of the storm. Example wind fields at three time steps are shown in Figure 7.

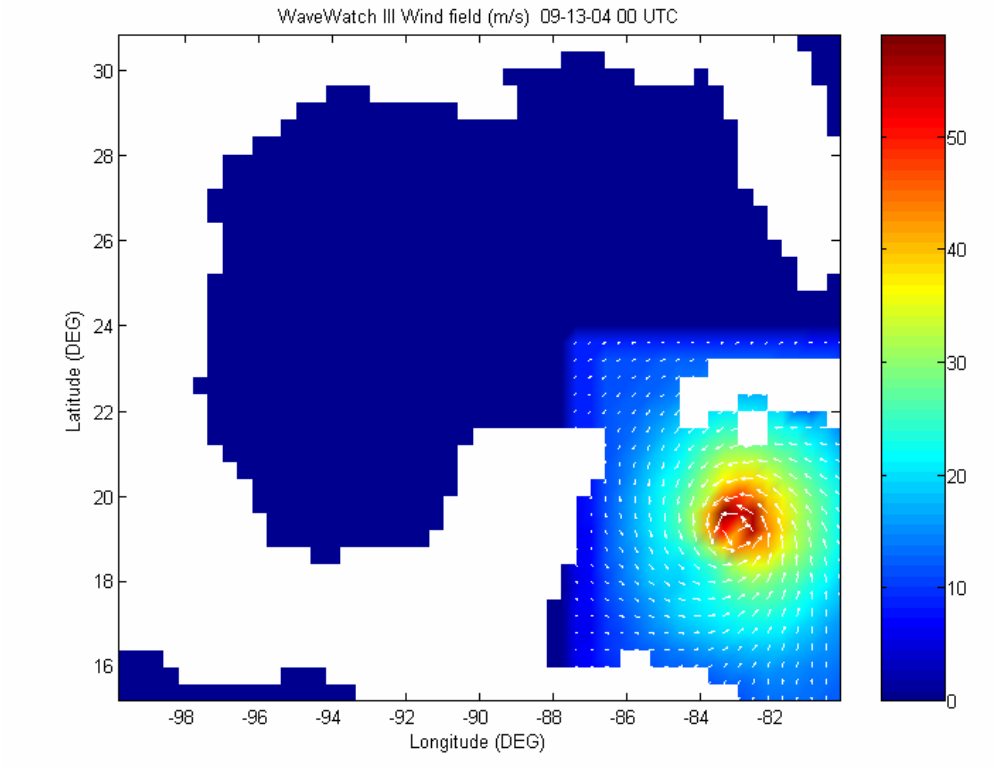
WaveWatch III Wind field (m/s) 09-13-04 00 UTC
Latitude (DEG)
Longitude (DEG)
30
28
26
24
22
20
18
16
-98
-96
-94
-92
-90
-88
-86
-84
-82
50
40
30
20
10
0

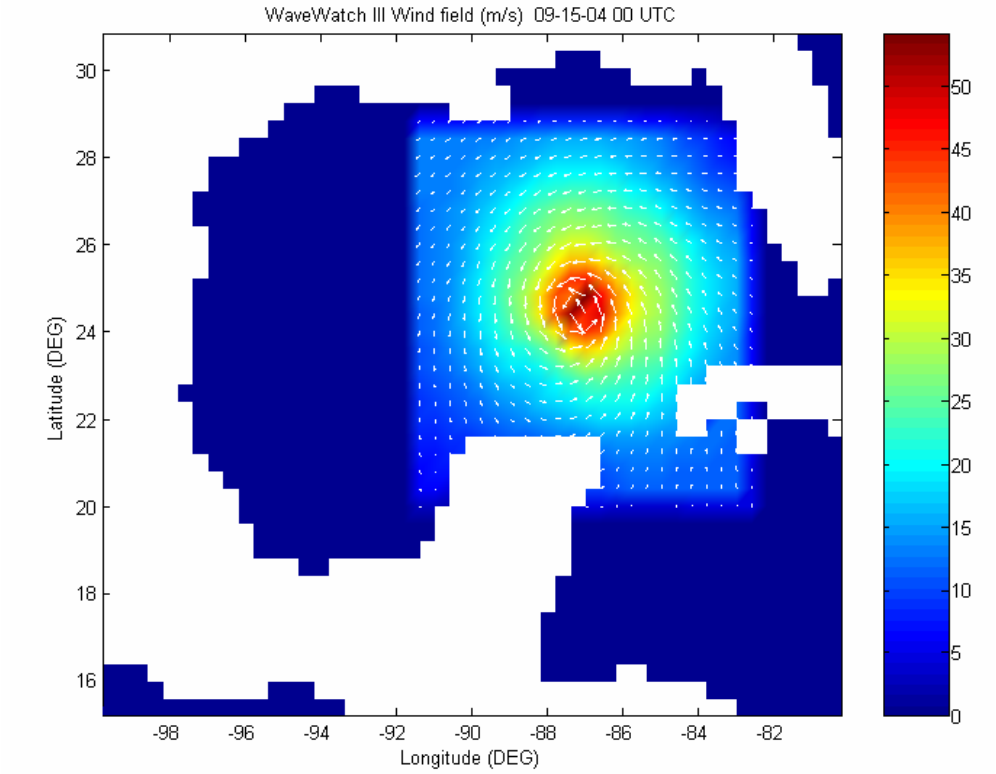
WaveWatch III Wind field (m/s) 09-15-04 00 UTC
Latitude (DEG)
Longitude (DEG)
30
28
26
24
22
20
18
16
-98
-96
-94
-92
-90
-88
-86
-84
-82
50
45
40
35
30
25
20
15
10
5
0

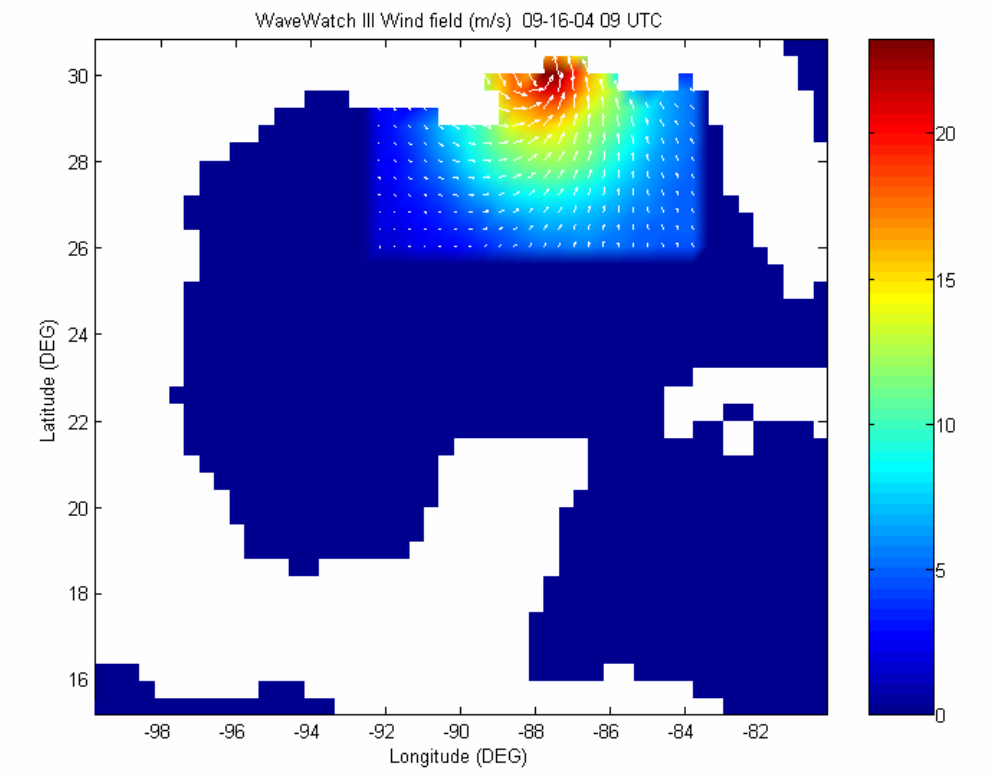

Figure 7. Example AOML H-Wind field snapshots during Ivan. The wind field is gridded on a moving "square" of approximately 1000Km by 1000Km centered on the eye of the storm

IV. WAVE MODEL

A. BRIEF DESCRIPTION OF WAVEWATCH III (WW3)

WAVEWATCH III (WW3) is a full-spectral third-generation wind wave model developed at the Marine Modeling and Analysis Branch (MMAB) of the Environmental Modeling Center (EMC) of the National Centers for Environmental Prediction (NCEP). It is based on previous versions of the same model with improvements in coding structures, numerical methods and physical parameters. WAVEWATCH III version 2.22 (Tolman, 2003) was used for the hindcasts in this thesis.

WAVEWATCH III solves the spectral wave action balance equation for wavenumber-direction density spectra. The implicit assumption of this equation is that properties of the medium (water depth and current) as well as the wave field itself vary on time and space scales that are much larger than the variation scales of a single wave. A further constraint is that the parameterizations of physical processes included in the model do not address conditions where the waves are strongly depth-limited. These two basic assumptions imply that the model can generally be applied on spatial scales (grid increments) larger than 1 to 10 km, and outside the surf zone (http://polar.ncep.noaa.gov/waves/wavewatch).

The wave action balance is given by:

$$\frac{DN}{Dt} = S = S_{in} + S_{nl} + S_{ds} + S_{bot} \qquad (1)$$

The left hand side represents the total derivative (moving with a wave component) of the action density spectrum N and S stands for the net effect of sources and sinks. This net effect of sources in WW3 is represented as a superposition of wind input (S_{in}), non-linear transfer (S_{nl}) and dissipation (S_{ds}). In order to extend its application to shallow coastal water, an additional bottom friction source term (S_{bot}) is included.

Modifications and empirical fine-tuning of the source terms has led to several alternative formulations. In this study the more recent formulation, proposed by Tolman and Chalikov (1996), was used. This source term package consists on an input source, and two dissipation components.

The input and dissipation terms, S_{in} and S_{ds}, are treated as a collective source term, since they are inter-connected (Tolman, 2002). The parameterization used is based on the fact that the dissipation processes for frequencies at and below the spectral peak are different from those occurring at high frequencies. For this reason, the WAVEWATCH III dissipation term contains two different components, one for low frequencies, $S_{ds,l}$, dominated by turbulence and another one for high frequencies, $S_{ds,h}$, representing the losses by whitecapping.

Nonlinear wave-wave interactions, S_{nl}, were modeled using a Discrete Interaction Approximation (DIA) method (Hasselmann et al., 1985).

The bottom friction parameterization is based on an empirical relationship from the Joint North Sea Wave Project (JONSWAP) study.

B. GRID SETTINGS

For this study two grids were used. A large scale, relatively coarse grid with 0.2° spatial resolution covers the entire Gulf of Mexico and surrounding areas between parallels 15°N and 31.2°N and meridians 100°W and 79.8°W. A fine resolution (0.05˚) grid was implemented for the eastern part of the Gulf of Mexico between parallels 21° and 31° North and meridians 93° to 80° West. High resolution bathymetry from the National Geophysical Data Center (NGDC) was used to accurately resolve coastline and bathymetry effects in the area of the SAX04 experiment. The spectral calculations for both grids were computed along 24 directions spanning the full circle (every 15˚) and 30 frequencies between 0.0412 Hz and 0.6530 Hz.

The wind field was interpolated in order to match the wave model resolution while the bathymetry was rearranged.

THIS PAGE INTENTIONALLY LEFT BLANK

V. WAVE MODEL – DATA COMPARISONS

In order to raise our understanding of the variability in wave conditions observed during Ivan as well as to test the accuracy of the WaveWatchIII model, several model runs were made and the outputs were compared with the different sets of in situ data that were collected by the NDBC buoy network and in the SAX04 experiment, as well as the GFO satellite altimeter data. Basically, comparisons were divided in two areas; Deep and Shallow water. The deep water area covered the entire Gulf of Mexico with a relatively coarse, 0.2˚ degree, spatial resolution. Here the wave-bottom interactions are non-existent, so there is no gain in increasing spatial resolution. However, in the shallow water area of the SAX04 Experiment wave-bottom interactions become of main interest, so, a finer resolution (0.05˚ degree) grid covering the eastern side of the Gulf was used to resolve the bathymetry and the coastline as well.

Dissipation by bottom friction is a very important mechanism when comparing data in shallow water. In order to understand how much energy is dissipated by this process and how well WW3 accounts for it, model runs with and without dissipation were compared.

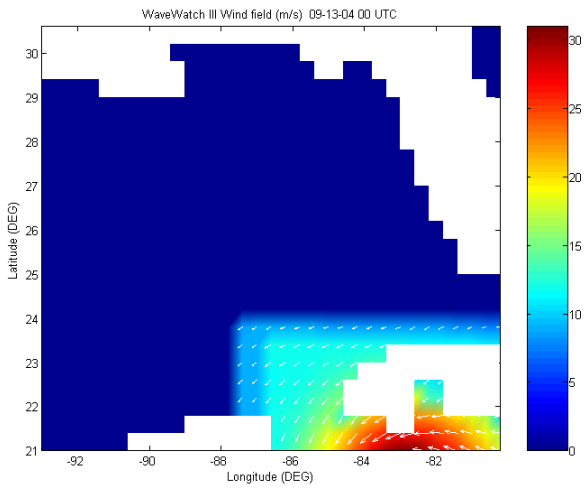
WaveWatch III Wind field (m/s) 09-13-04 00 UTC
Latitude (DEG)
Longitude (DEG)

a)

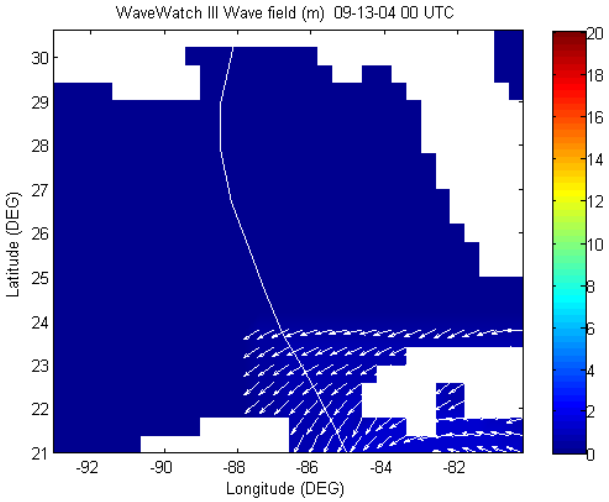
WaveWatch III Wave field (m) 09-13-04 00 UTC
Latitude (DEG)
Longitude (DEG)

b)

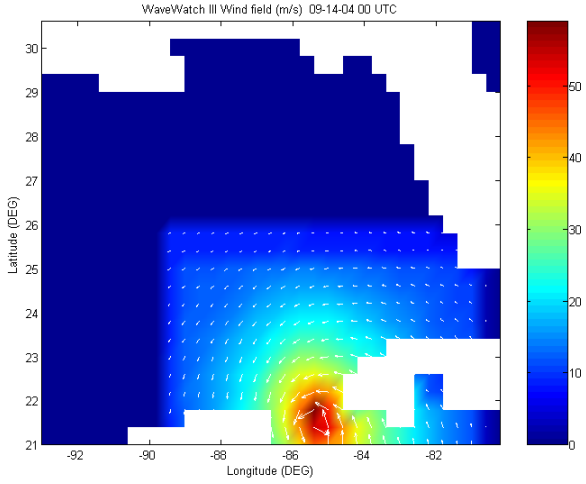
WaveWatch III Wind field (m/s) 09-14-04 00 UTC
Latitude (DEG)
Longitude (DEG)

c)

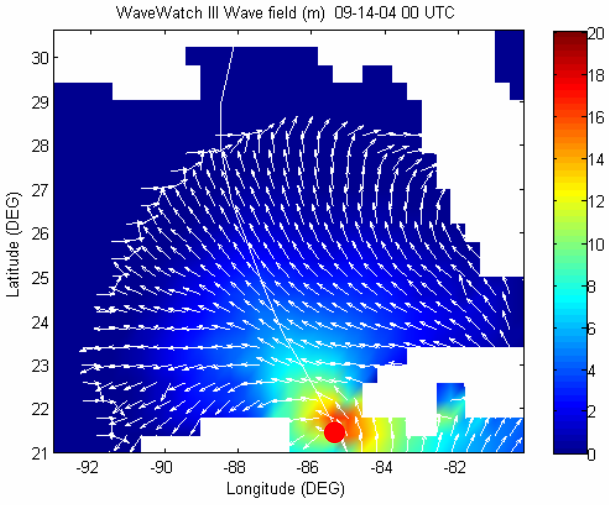
WaveWatch III Wave field (m) 09-14-04 00 UTC
Latitude (DEG)
Longitude (DEG)

d)

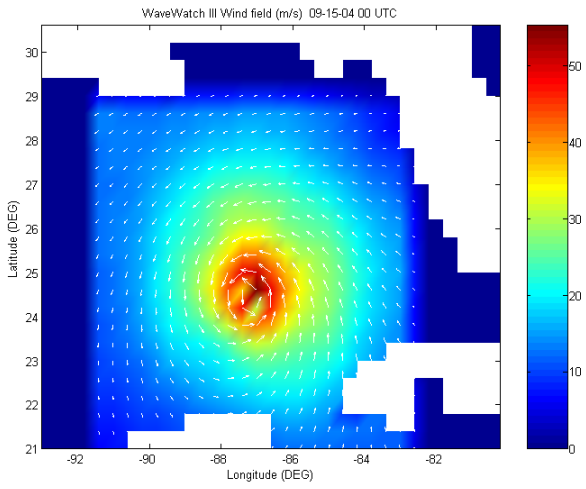
WaveWatch III Wind field (m/s) 09-15-04 00 UTC
Latitude (DEG)
Longitude (DEG)

e)

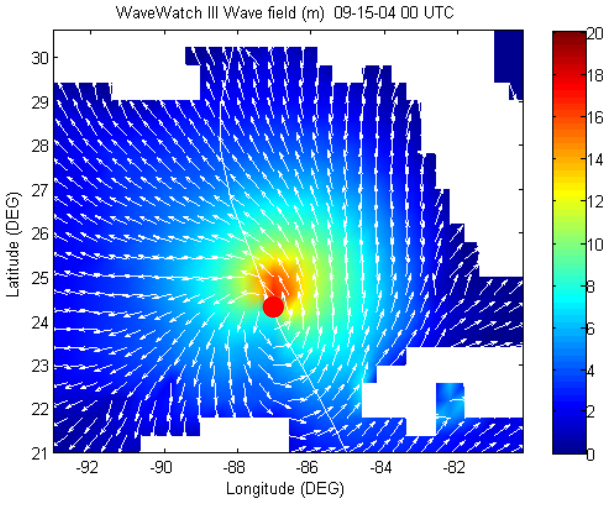
WaveWatch III Wave field (m) 09-15-04 00 UTC
Latitude (DEG)
Longitude (DEG)

f)

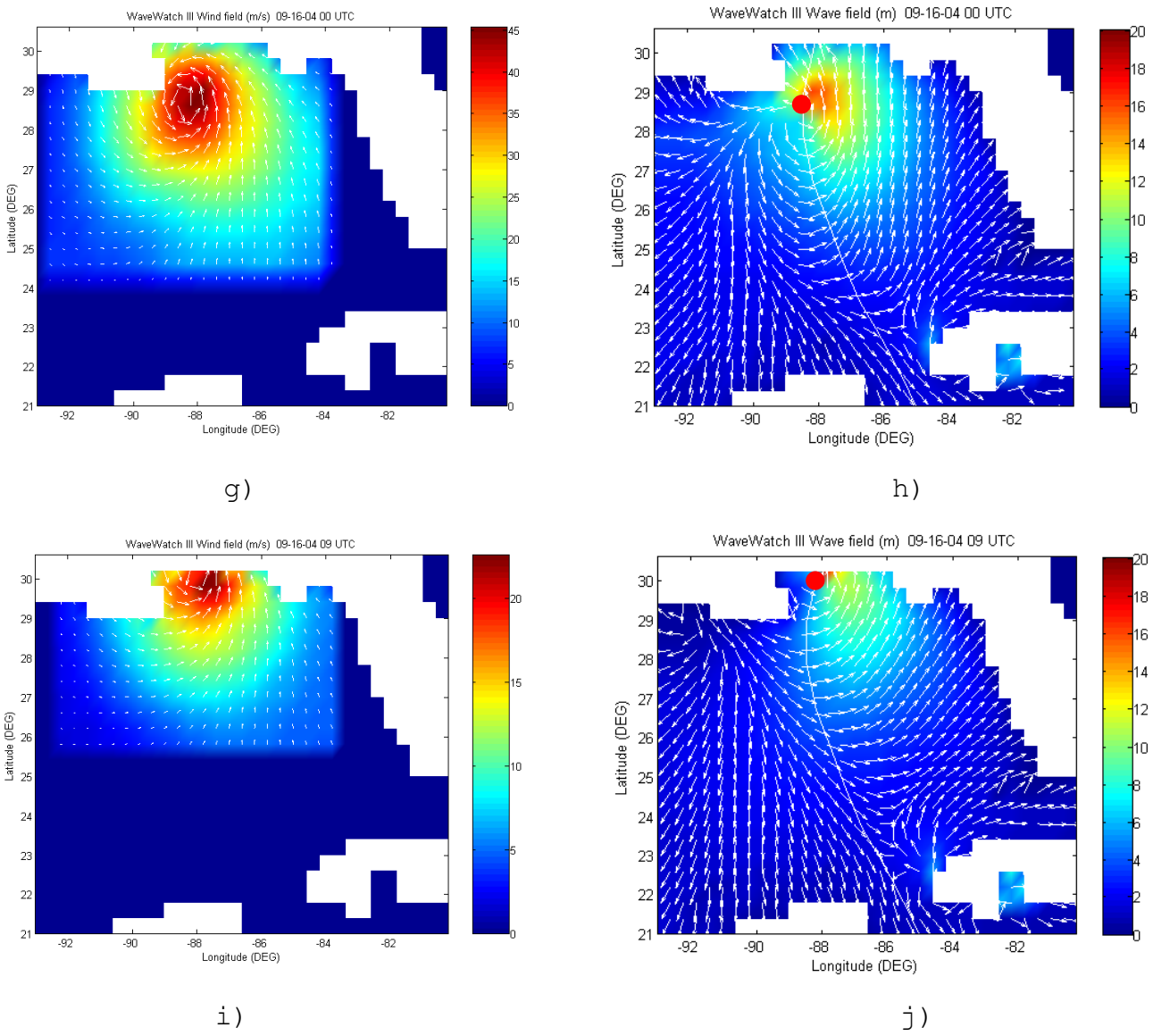

Figure 8. The left column shows the synoptic wind field and the right column the corresponding wave field for Sep. 13 00:00 UTC, 14 00:00 UTC, 15 00:00 UTC, 16 00:00 UTC and 16 09:00 UTC (landfall). The white line indicates hurricane track with a red filled circle at the location of the hurricane eye. The white arrows indicate the wind (left panels) and wave (right panels) directions. Colors correspond to wind speed (left panels) and significant wave height (right panels).

A. DEEP WATER

Before describing the deep water model-data comparisons, it is useful to give a synoptic description of the predicted evolution (Figure 8). Since the AOML H-winds grid only covers a square area of approximately 1000 Km by 1000 Km, the forcing that generates waves in WW3 is confined to this area.

The Gulf of Mexico is practically isolated from the Atlantic Ocean and from the Caribbean Sea as well. The only significant opening where swell can enter the Gulf is the Yucatan Channel (around 200 Km wide). No significant wave activity is predicted in the Gulf until the storm covers the Yucatan Channel (Figure 8).

After this point, waves have the entire Gulf to grow and expand. In less than 24 hours, waves reach a height of 20 meters. As the storm reaches the northern half of the Gulf, a marked asymmetry between the wave field on the right and left side of the hurricane track develops. On the right side (East) of the hurricane track, the waves are propagating in the same direction as the storm, allowing the waves to spend more time under the storm influence resulting in higher waves. On the other hand, on the left side, waves are propagating away from the storm resulting in smaller waves.

As described in chapter 2, seven NDBC buoys were chosen for comparisons. Model-data comparisons of the bulk parameters, Significant Wave Height (SWH), Mean Wave Direction (MWD) and Peak Period (Tp) are shown in Figures 9-11.

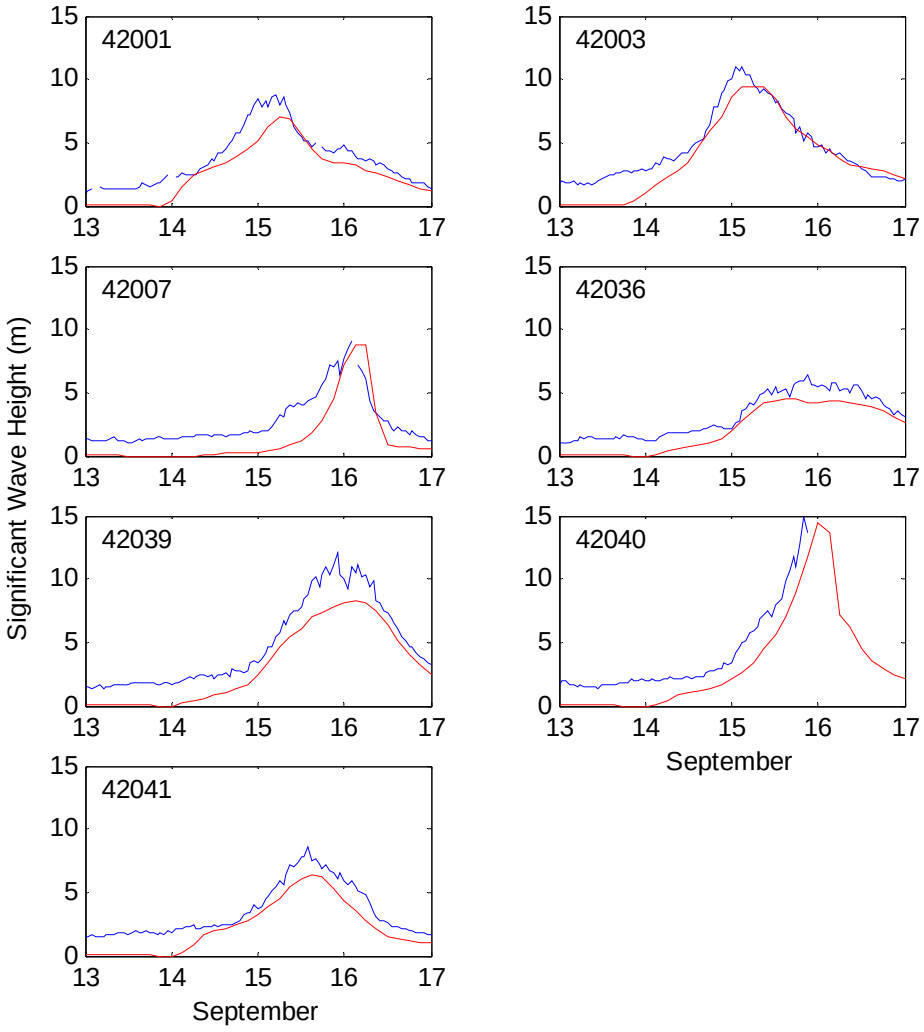

Figure 9. Comparison of observed (blue curve) and predicted (red curve) significant wave heights at the seven NDBC buoys.

Since the seven buoys are all located in the northern half of the Gulf, no significant wave activity (SWH close to zero) is predicted on the first day (September 13) when the storm enters the Gulf (Figure 9). The observed SWH reflect local atmospheric forcing that is not accounted for in the WW3 predictions. There is a notable time difference

between when maximum wave heights were observed versus the WW3 prediction. After the storm passes by and the wave heights start to decrease, WW3 predictions agree reasonably well with the observations. Buoy 42040 was damaged during the passage of the hurricane and did not report data during the waning stage of the storm.

The predicted mean wave directions are in reasonable agreement with the observations (Figure 10). Predictions at buoys 42001 and 42003 capture the observed direction inversions as the storm passes by, with waves first arriving from East quadrants and then turning to North or Northwest.

To describe the directional wave field in more detail, predictions of the frequency-directional wave spectra during and after the storm passage are compared in Figures 11 and 12. At station 42001, on the West side of the storm, the energy at lower frequencies arrives from the East spreading to the northern quadrants at higher frequencies. This pattern is consistent with the cyclonic wind circulation (Figure 11-a). Whereas the lower frequency swell responds to forcing over several days from the predominant easterly winds, the high frequency part of the spectrum quickly adjusts to the local wind direction, which is from the North. Later on September 16 (Figure 11-b), the storm had already made landfall, and the wind has been blowing from North with a restricted fetch. The energy is concentrated at higher frequencies and arrives from the northern quadrants, with a smaller residual swell from the east.

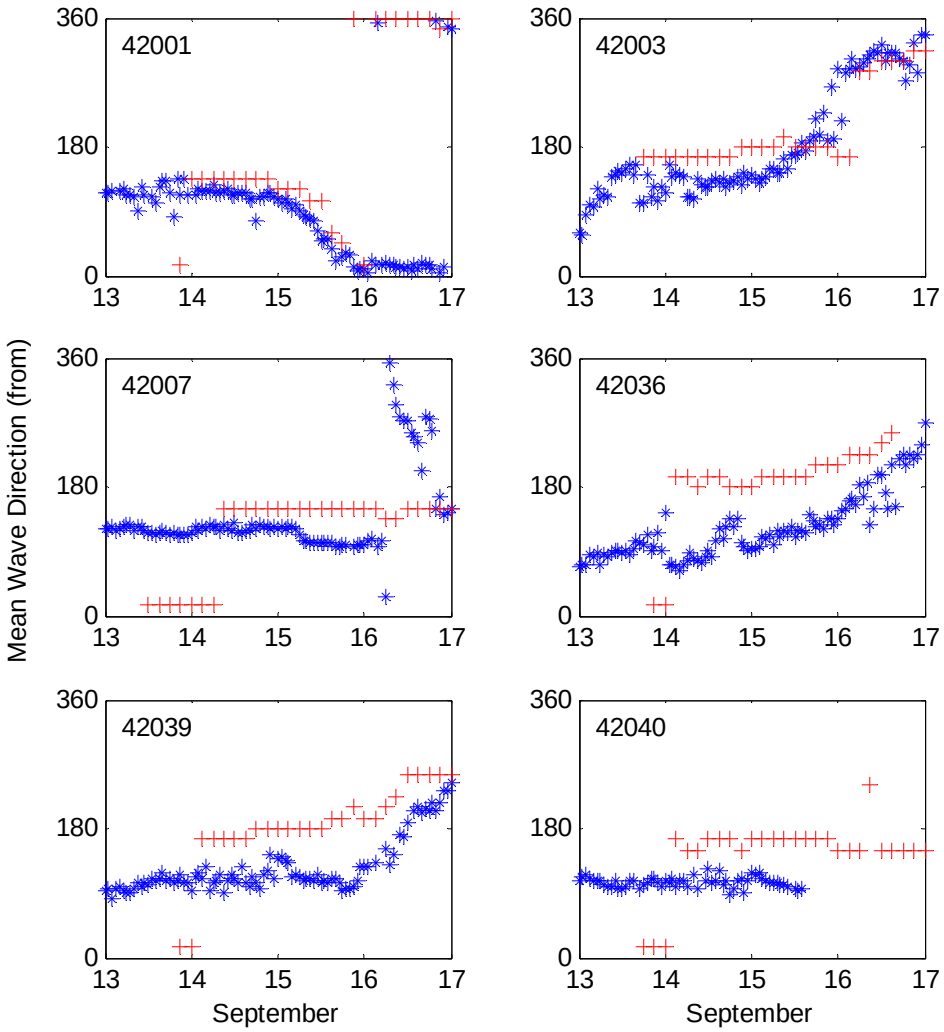

Figure 10. Comparison of the observed (blue crosses) and predicted (red crosses) mean wave direction at six NDBC buoys.

On the other hand, at station 42003 located on the East side of the storm, (Figure 12-a), the dominant low frequency wave energy during the storm passage arrives from the south. Later, as the storm made landfall, (Figure 12-b) the energy distribution is similar to that predicted at

station 42001, but with low frequency residual swell arriving from the northwest, again consistent with the cyclonic circulation.

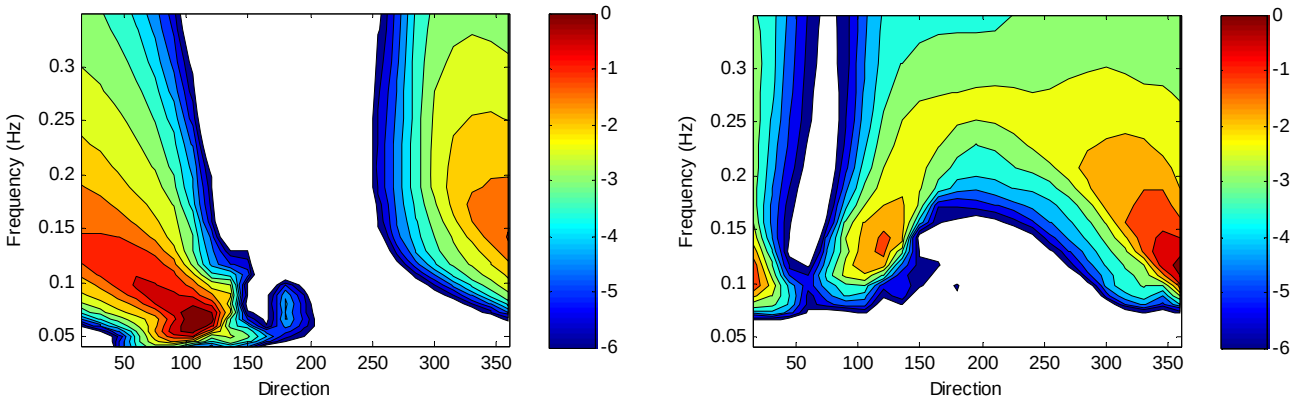

a) b)

Figure 11. Two-dimensional frequency-directional spectra predicted by WW3 at station 42001. a) 15SEP 09:00UTC; b) 16SEP 15:00 UTC. Contours indicate energy levels on a log scale at $10^{1/2}$ intervals relative to the maximum energy.

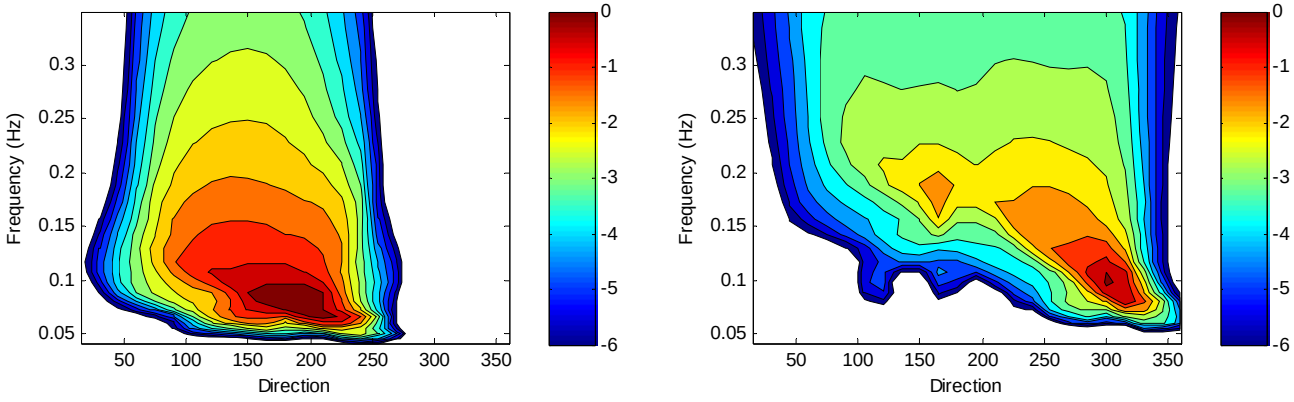

a) b)

Figure 12. Two-dimensional frequency-directional spectra predicted by WW3 at station 42003. a) 15 SEP 09:00UTC; b) 16SEP 15:00 UTC. Contours as in previous figure.

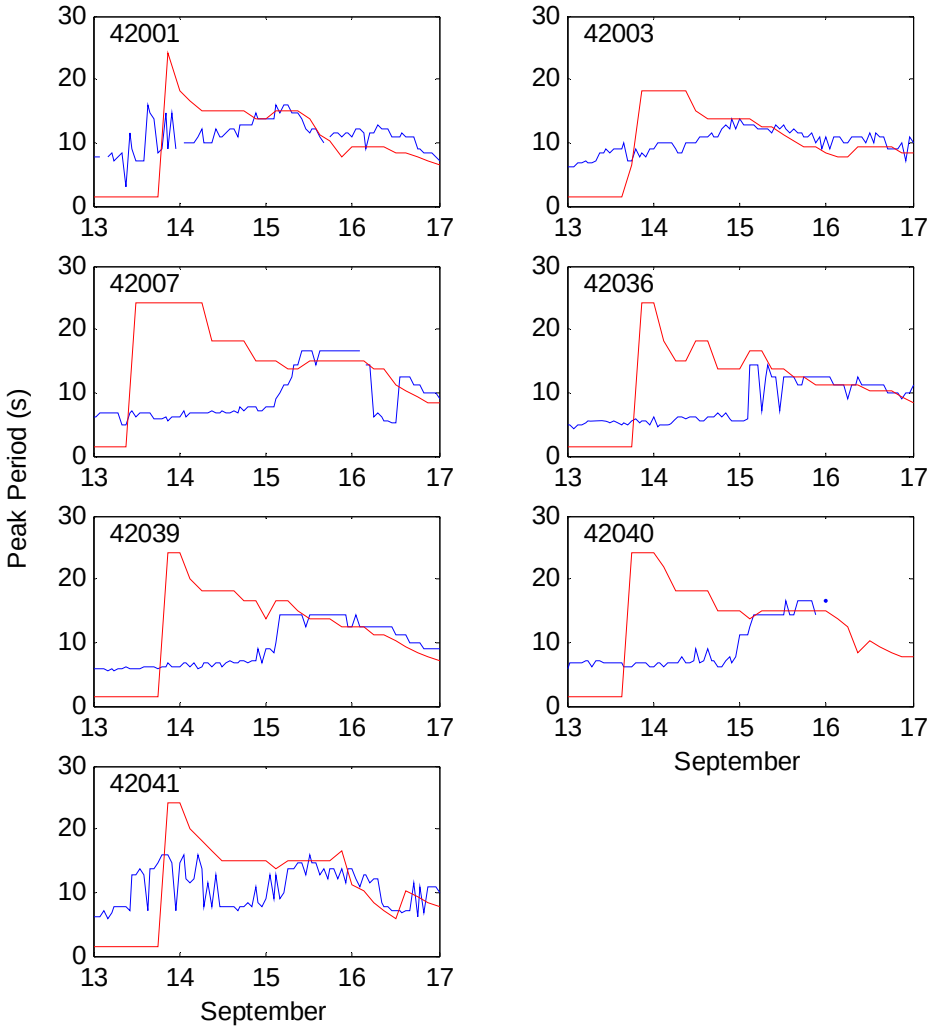

Figure 13. Comparison of observed (blue curve) and predicted (red curve) peak period at the seven NDBC buoys.

Regarding the peak period (Figure 11), on September 13 and 14 there are large differences between the model predictions and observations. The model predicts very low frequency (and low energy) waves that are the forerunners of Ivan whereas the observed wave field at the NDBC buoys is still dominated by higher-frequency locally generated seas (not accounted for in the WW3 hindcast). The agreement

between observations and predictions improves dramatically on the latter two days when the large waves from Ivan reach the buoys.

The satellite altimeter measurements allow for additional WW3 model verification in regions of the Gulf of Mexico where there are no NDBC buoys. Observed and predicted significant wave height along seven satellite tracks that overlap the model domain (Figure 14) are compared in Figure 15. Results confirm the earlier noted model tendency to underpredict SWH.

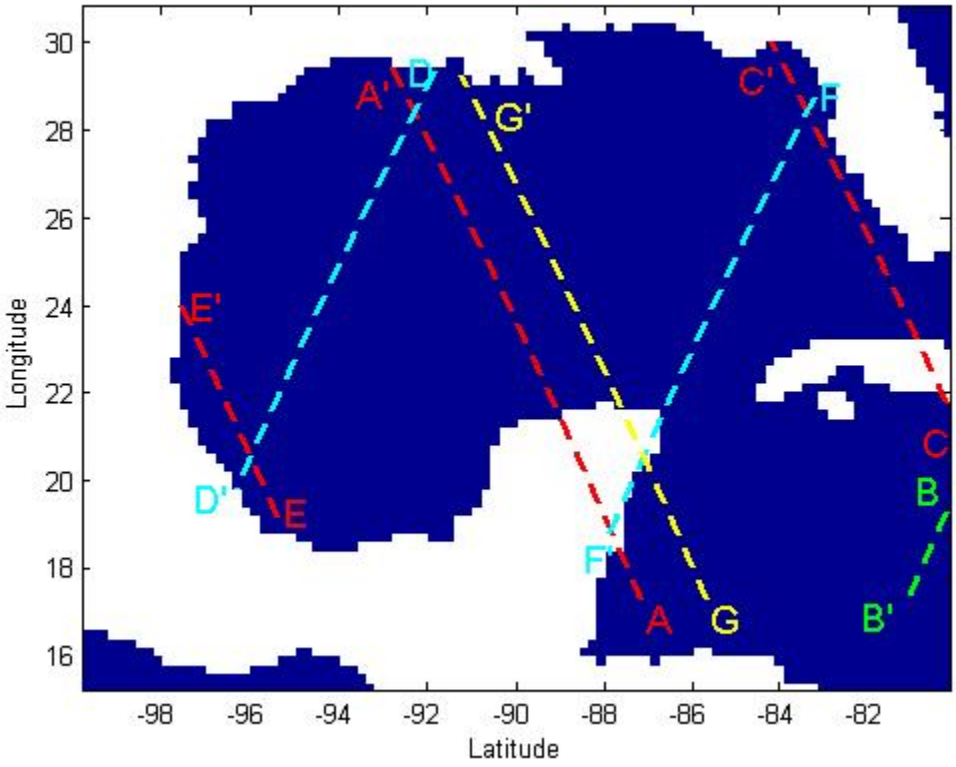

Figure 14. GEOSAT FOLLOW ON (GFO) satellite tracks – September 13-16, 2004

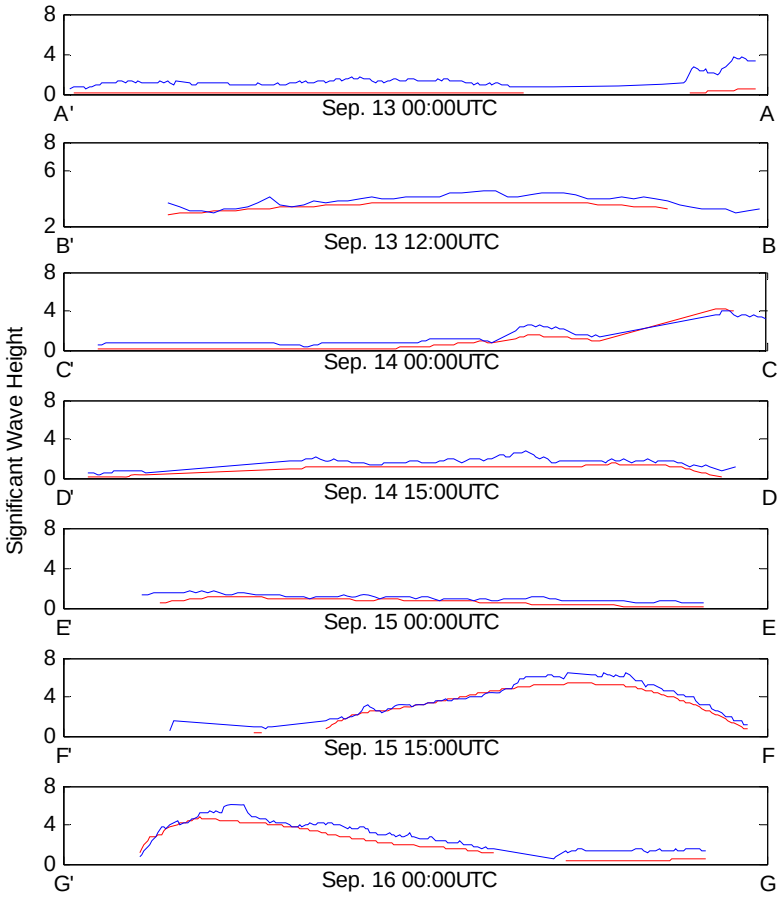

Figure 15. Comparisons between GEOSAT observations and WaveWatch III predictions along the tracks shown in Figure 14.
Red line – WW3 predictions
Blue line – GEOSAT measurements

B. FLORIDA CONTINENTAL SHELF

To resolve coastal boundary and bathymetry effects, a high resolution (0.05˚ degree) grid was implemented for the Eastern part of the Gulf including the Florida panhandle shelf where the SAX04 measurements were colleted. To

investigate the importance of dissipation (bottom friction) on the continental shelf and evaluate the empirical JONSWAP parameterization used in WW3, model runs were performed both with and without bottom friction.

The area where Hurricane Ivan made landfall features a complex coastline. From Venice, LA to Panama City, FL, the coastline is highly irregular with a chain of barrier islands and a complex inner shelf. The barrier islands south of Pensacola and Fort Walton Beach form a perfect natural wave barrier. Since nearshore processes (i.e. storm surge and surf zone wave breaking) are not accounted for in WW3, the model computations were restricted to areas deeper than 5 meters.

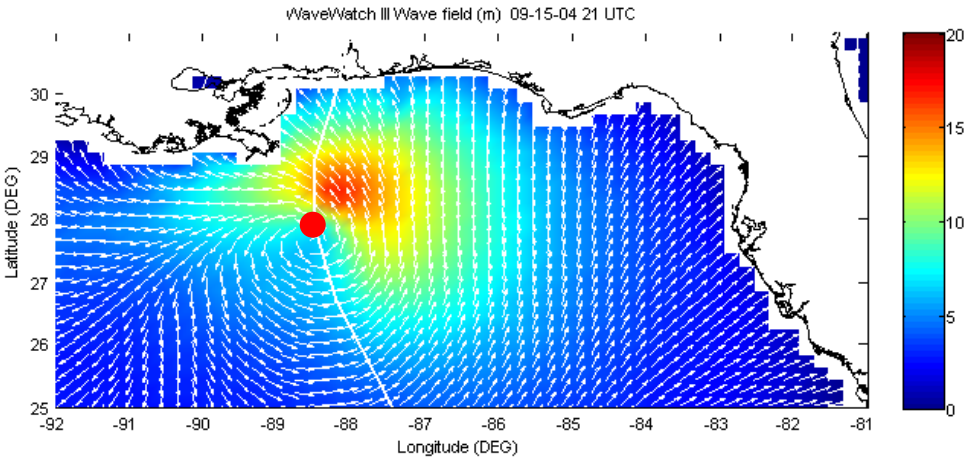

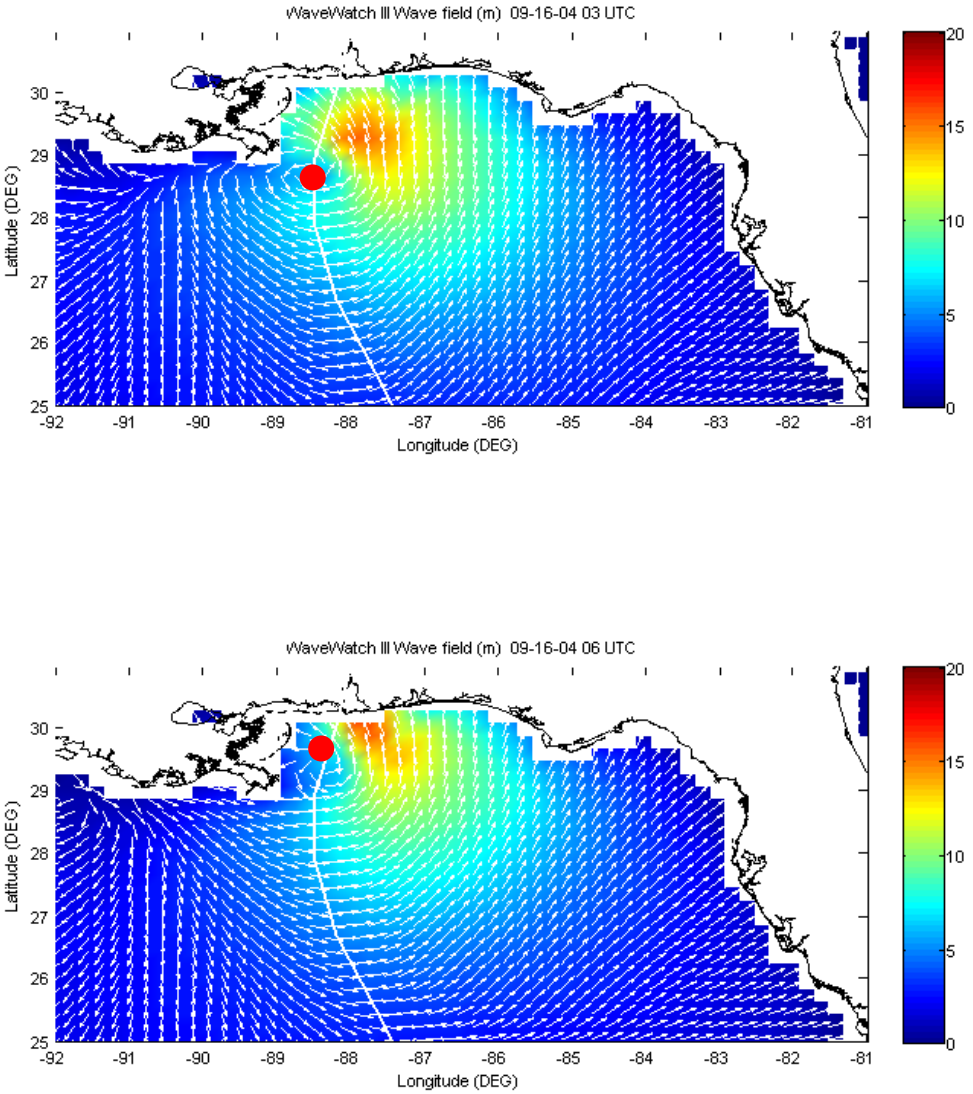

Figure 16. WW3 Wave field (SWH) predictions for September 15 21:00UTC and September 16, 03:00 and 06:00 UTC The Hurricane track is represented by the white line and the red spot indicates the eye of the storm.

The Highest SWH is predicted to the east and ahead of the storm center. As discussed earlier, on the east side, waves propagate along with the storm thus increasing the "dwell time" when waves are under the influence of hurricane force winds. Since group speed of the dominant

waves is large than the speed with which the storm advances, the largest waves are found slightly ahead of the storm center. On the west side, waves propagate away from the storm, minimizing the time that they are under the storm influence, resulting in lower wave heights.

Comparing these high-resolution synoptic fields with the earlier discussed coarser resolution run, the differences between the predicted mean wave directions are surprisingly small even in the shallow shelf areas. These results indicating that refraction effects are weak. On the right side of the hurricane track, the unlimited fetch drives long period waves that feel the bottom across the entire shelf, but these waves propagate northward almost perpendicular to the bathymetry, minimizing the refraction effects. On the other hand on the left side of the storm, waves propagate southeastward, and since the wind is blowing offshore the fetch is very limited, resulting in high frequency waves that also are not strongly affected by refraction (Figure 17).

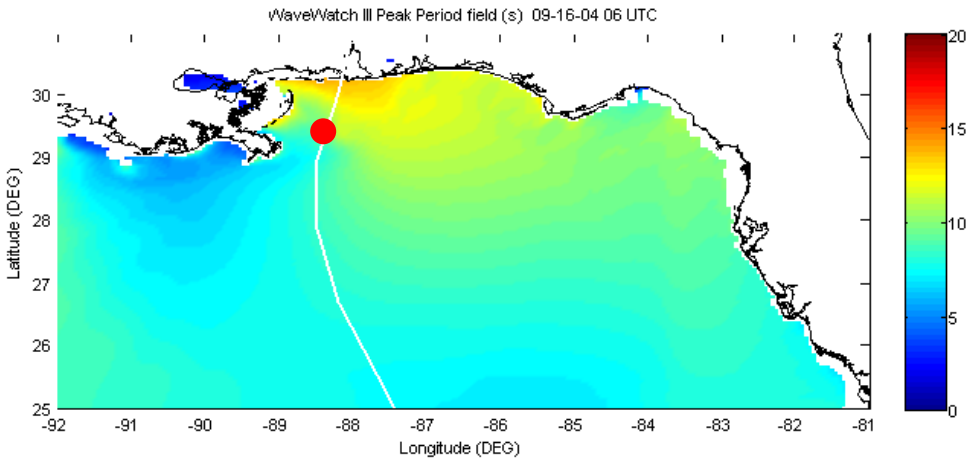

Figure 17. WW3 Peak Period field. The Hurricane track is represented by the white line while the red spot indicates the eye of the storm.

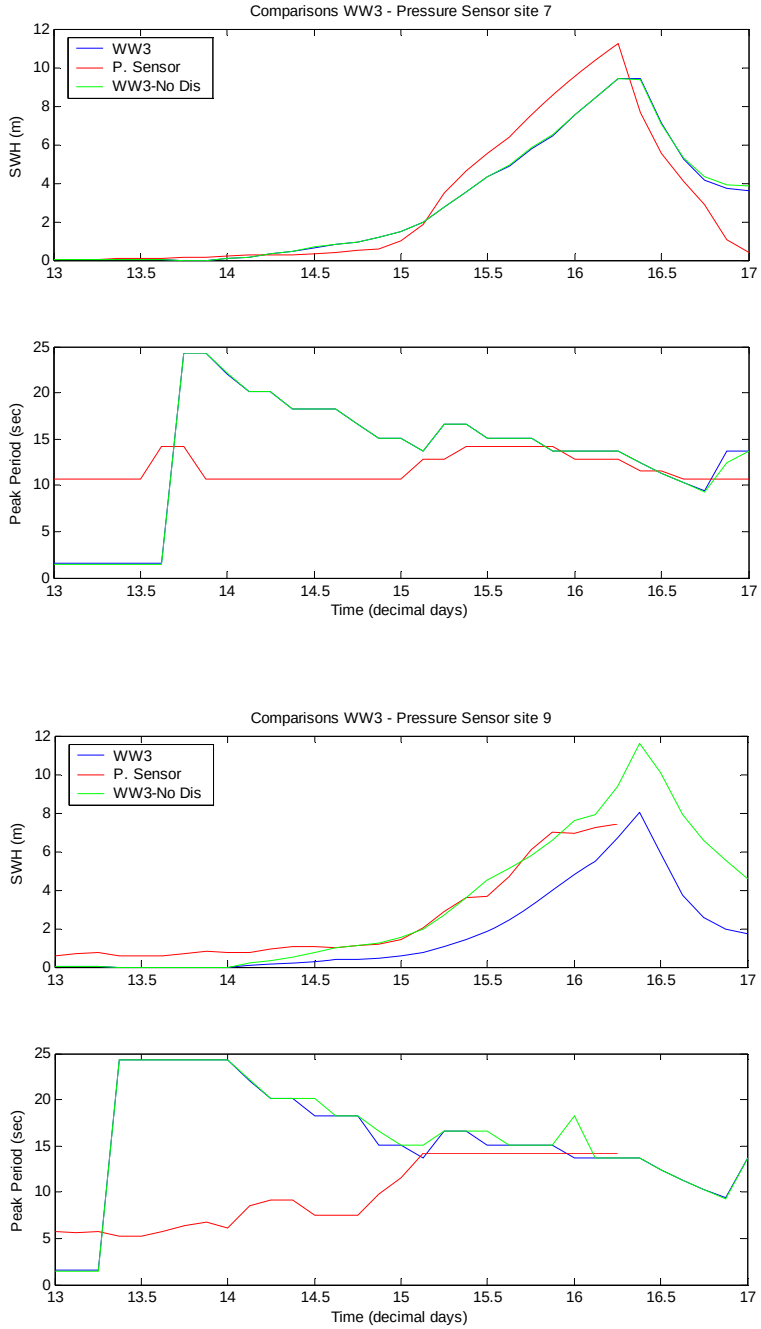

Figure 18. Comparison between WW3 predictions and observations at SAX04 sites 7 and 9. Blue line – WW3 predictions with dissipation
Red line – SAX04 instruments observations
Green line – WW3 predictions without dissipation

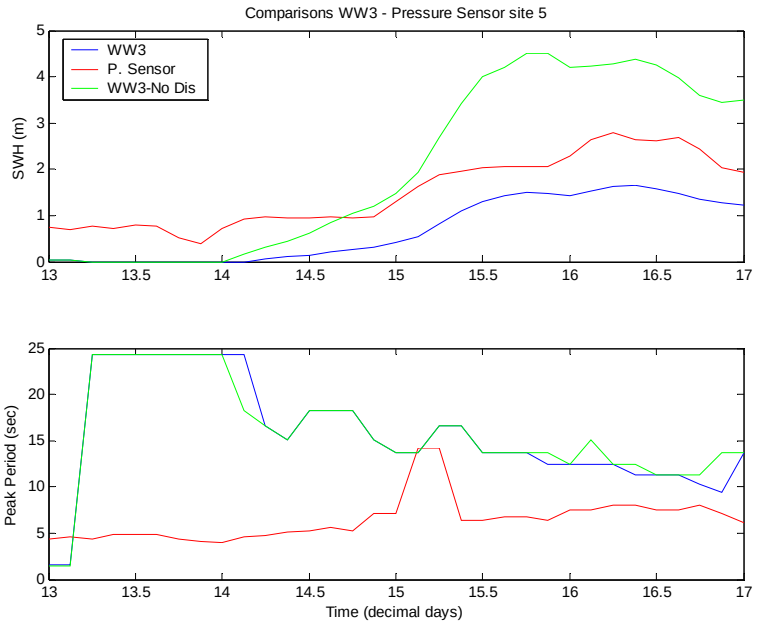

Figure 19. Comparison between WW3 predictions and observations at SAX04 site 5.
Blue line – WW3 predictions with dissipation
Red line – SAX04 instrument observations
Green line – WW3 predictions without dissipation

At SAX04 site 7 (83 meters depth – Figure 18) the WW3 predictions with and without dissipation are practically identical, indicating that bottom friction in these relatively deep regions is negligible. On the other hand, at site 9, WW3 predictions without dissipation match the actual in situ observations almost perfectly whereas predictions with dissipation are biased low by about 40%. Although it is possible that WW3 is dissipating too much energy, the agreement without dissipation must be fortuitous, since the large waves propagating through this shallow region are approaching depth-limited wave breaking.

Overall, these comparisons indicate that the wave decay by bottom friction is relatively weak across this narrow section of the continental shelf.

At site 5, inshore of the wide shelf of Apalachee Bay, WW3 predicts large differences in wave heights with and without dissipation, consistent with the strong dissipation expected across a wide shelf. The model without dissipation overpredicts the SWH by almost a factor of 2 whereas the model with dissipation underpredicts the SWH by about 30%, suggesting that the default setting for dissipation induced by bottom friction in WW3 is too high for these conditions.

THIS PAGE INTENTIONALLY LEFT BLANK

VI. CONCLUSIONS

The objective of this study was to test the performance of the operational wave prediction model WaveWatch III in regional applications under extreme meteorological conditions, such as hurricanes. Model hindcasts were performed for category V Hurricane Ivan which made landfall on the Alabama coast in 2004. Model predictions are compared with measurements collected in the ONR Sediment Acoustics Experiment SAX04 and data from NDBC buoys in the Gulf of Mexico and the Geosat Follow On Satellite.

Three model runs were made. One run, covering the entire Gulf of Mexico, with 0.2° degree spatial resolution and two runs, for the Eastern part of the Gulf, with 0.05° degree resolution, one with and one without dissipation. The model was forced with AOML H-winds.

Comparisons with seven NDBC buoys, 13 SAX04 instruments and GFO altimeter data were made for the period of September 13 to September 16, 2004, while Hurricane Ivan crossed through the Gulf of Mexico.

In deeper areas, analysis reveals that WaveWatchIII has a tendency to underpredict wave heights and to be consistently late (about four to six hours) in predicting the arrival of the dominant waves. On the other hand, the predicted decaying phase of the wave evolution matches the observations fairly well. In shallow areas, the model predicts too much dissipation.

The model predicts large differences between wave conditions on the left and right sides of the hurricane path owing to the difference in “dwell time” between waves

propagating against and with the storm. The reduced fetch on the left side of the storm limits the wave growth during landfall.

Overall, the WaveWatchIII hindcasts are in reasonable agreement with the observations.

LIST OF REFERENCES

Hasselmann, K. et al, 1973, Measurements of wind-wave growth and swell decay during the Joint North Sea Wave Project (JONSWAP), Dtsch. Hydrogh. Z, Suppl. A

Hasselmann, S, and K. Hasselmann, Computations and parameterizations of the nonlinear energy transfer in a gravity wave spectrum. Part I: a new method for efficient computations of the exact nonlinear transfer integral. *Journal of Physical Oceanography,* v15, 1369-77, 1985.

Liu, W.T., K.B. Katsaros and J.A. Businger, Bulk parameterizations of air–sea exchanges of heat and water vapor including the molecular constraints at the interface, *Journal of Atmospheric Science,* v36, 1722–1735, 1979.

Powell, M. D., S. H. Houston and T. A. Reinhold, Hurricane Andrew's Landfall in South Florida. Part I: Standardizing Measurements for Documentation of Surface Wind Fields, *Weather Forecasting*, v11, pp. 304-328, 1996.

Steele, K.E. and T.R. Mettlach, NDBC wave data - current and planned. *Ocean Wave Measurement and Analysis - Proceedings of the Second International Symposium*. ASCE, pp. 198-207, 1993.

Stewart, Stacy R., Hurricane Ivan 2-24 September 2004 - Tropical Cyclone Report, *National Hurricane Center,* 2005.

Sverdrup, H.U. and W.H. Munk, *Wind,* Sea, and Swell: Theory of Relations for Forecasting. *U.S. Navy Dept, Hydrographic Office*, H.O. Pub. No. 601, 44 pp, 1947.

Tolman, L, Numerical Simulation of Sea Surface Directional Wave Spectra under Hurricane Wind Forcing, *Journal of Physical Oceanography, v33, pp 1680-1706, 2003.*

Tolman, L. and Dmitry Chalikov, Source Terms in a Third-Generation Wind Wave Model, *Journal of Physical Oceanography,* v26, pp 2497-2518, 1996.

Tolman, H.L., User manual and system documentation of *WAVEWATCHIII* version 2.22. *WAVEWATCH III,* U.S. Department of Commerce, National Oceanic and Atmospheric Administration, National Weather Service, Technical Note, September 2002.
[www.polar.wwb.noaa.gov/waves/wavewatch/wavewatch.html]

WAMDI group, The WAM model - a third generation ocean wave prediction model. *Journal of Physical Oceanography,* v18 pp 1775-1810, 1988.

INITIAL DISTRIBUTION LIST

1. Defense Technical Information Center
   Ft. Belvoir, Virginia

2. Dudley Knox Library
   Naval Postgraduate School
   Monterey, California

3. Professor Mary L. Batteen
   Department of Oceanography
   Naval Postgraduate School
   Monterey, California

4. Professor Thomas Herbers
   Department of Oceanography
   Naval Postgraduate School
   Monterey, California

5. Professor Edward B. Thornton
   Department of Oceanography
   Naval Postgraduate School
   Monterey, California

6. Mr Paul Jessen
   Department of Oceanography
   Naval Postgraduate School
   Monterey, California

7. Director-Geral do Instituto Hidrográfico
   Instituto Hidrográfico
   Rua das Trinas, 49
   Lisboa - PORTUGAL

8. CDR Carlos Ventura Soares
   Instituto Hidrográfico
   Rua das Trinas, 49
   Lisboa - PORTUGAL